Alexander Hoer, Fabian Gapp, Franziska Wanka

Revealing the Hidden Urban Landscape of Munigua: Insights from the 2024 Ground-Penetrating Radar Survey and Its Implications for Roman and Post-Roman Occupation

Madrider Mitteilungen Bd. 66 (2025) 254-275

https://doi.org/10.34780/0h8kn659

Herausgebende Institution / Publisher:
Deutsches Archäologisches Institut

ABSTRACT

Revealing the Hidden Urban Landscape of Munigua

Insights from the 2024 Ground-Penetrating Radar Survey and Its Implications for Roman and Post-Roman Occupation

Alexander Hoer – Fabian Gapp – Franziska Wanka

The 2024 ground-penetrating radar (GPR) survey at the Roman city of Munigua has revealed new architectural structures, clarified spatial sequences, and expanded the known extent of urban development. Covering four key areas across the site, the high-resolution survey allowed for the identification of wall remains, layout variations, and transformations from the Roman through to the post-Roman period. Notably, one structure appears to have been reused or reconstructed during the early medieval period marking the first architectural trace of this phase. The results confirm the effectiveness of GPR in complex archaeological environments and contribute substantially to our understanding of Munigua's long-term urban dynamics.

KEYWORDS

Roman urbanism, Munigua, Ground-penetrating radar, Post-Roman transformation

Revealing the Hidden Urban Landscape of Munigua

Insights from the 2024 Ground-Penetrating Radar Survey and Its Implications for Roman and Post-Roman Occupation

1 Introduction

1 The archaeological research in Munigua has a long history. The site was first documented in 1565 by Alonso Chacón and Ambrosio de Morales, and the first scientific investigations were carried out in the 18th century (1756) by Sebastián Antonio de Cortés and José de las Cuentas Zayas. In 1921, the French archaeologist Pierre Paris obtained an excavation permit but was unable to carry out any fieldwork due to a lack of resources[1].

2 A turning point in research at Munigua came in 1956, when the Andalusian heritage conservator Felix Hernández brought the site to the attention of the German Archaeological Institute (DAI) in Madrid[2]. Shortly thereafter, a team from the institute visited the site and, later that year, conducted the first archaeological prospection. Since then, systematic research has been carried out continuously, making Munigua a key reference site for the study of Roman provincial urbanism in the west[3]. Munigua has been inhabited since approximately the 5th century BCE as an Iberian settlement dedicated to iron smelting using locally extracted ore[4]. The site remained occupied during the Roman period, with metalworking first centred on copper and later returned to iron[5]. The preserved architectural remains date to the first two centuries CE, with the most extensive construction phase occurring around 70 CE. The Flavian period represents the city's heyday, during which Munigua likely received its municipal status, and most of its public buildings were constructed[6]. The scientific work on the site has led to the publication of over 100 specialized articles and several monographs[7]. Munigua is one of the most extensively studied ›small towns‹ in the Roman provinces, making it a site of major significance for research not only in Hispania. However, it also continuously

1 Schattner et al. 2017, 128 f.
2 Schattner 2007.
3 Schattner 2022, 242 f.
4 Griepentrog 2008, 327–332.
5 Schattner in press.
6 Schattner 2022, 245.
7 Cf. Krug 2018, 3–5.

challenges conventional perspectives on Roman urbanism. For example, despite its remote location in the Sierra Morena, a terraced sanctuary was constructed here following the architectural models of Latium[8]. The city exhibits an unusual concentration of public buildings, including multiple temples, bath complexes, a forum, and a two-story portico, which is striking given its small urban area of only 3.8 hectares within the city walls.

3 Adding to the uniqueness of Munigua is the fact that its necropoleis are located within the city walls – an exceptional phenomenon in the Roman world, where burial sites were traditionally placed outside urban limits[9]. The residential buildings, in contrast, are relatively modest in both size and number. Only about seven houses have been identified[10], and there appears to have been little space for many more. These factors contribute to the ongoing debate regarding Munigua's function, urban character, and the dynamics of its development within the broader framework of Roman provincial cities. To further explore these exceptional features and address unresolved questions regarding the city's layout and function, recent research has increasingly turned to geophysical prospection methods.

4 This article presents the results of the 2024 GPR survey, which builds on a long tradition of geophysical investigations at Munigua. As early as 2002, Thomas Schattner, in collaboration with Cornelius Meyer and Burkhart Ullrich from Eastern Atlas, successfully employed ground-penetrating radar (GPR) along the city wall and at the ›Casa de Alcántara‹ outside the urban area. In addition, geo-electrical surveys were conducted in the slag heaps of the copper and iron mines to estimate slag quantities[11]. Further geophysical prospections took place in 2013 and 2015, in cooperation with the Römisch-Germanische Kommission (Kerstin Brose and Roman Scholz), focusing on the southern slope of the urban area[12]. During these investigations, geo-electrical methods proved ineffective due to the low conductivity of the dry soil. Geomagnetic prospection also faced difficulties, as some anomalies were visible but difficult to interpret, likely due to the high content of iron slag in the ground. GPR, however, provided excellent results in this part of the urban area, proving to be the most effective prospection technique for detecting wall structures at the site.

5 Based on these experiences, a new GPR survey was conducted in 2024 under the direction of Alexander Hoer, in collaboration with Franziska Wanka and Fabian Gapp from the University of Erlangen. Given the success of previous campaigns, GPR was once again chosen as the primary method. The surveyed areas were distributed across the entire site but were limited to small, carefully selected zones (Fig. 1). The main objectives of the 2024 campaign were to better define the spatial extent of the city, identify new structures, and analyse changes in the urban layout within the context of Roman urbanism.

6 The following sections first provide an overview of the methodologies employed before presenting a detailed analysis of the results and their archaeological interpretation. A particular focus is placed on how the new data contributes to a revised understanding of Munigua's urban expansion, as well as its long-term transformation beyond antiquity.

8 Coarelli 1987; Schattner 2004.
9 Raddatz 1973; Vegas 1988; Kobusch 2010, 129; Kobusch 2014, 245–249.
10 Schattner 2019, 109 f. 115–122. 134–146.
11 Meyer et al. 2007.
12 Schattner et al. 2017, 140–142.

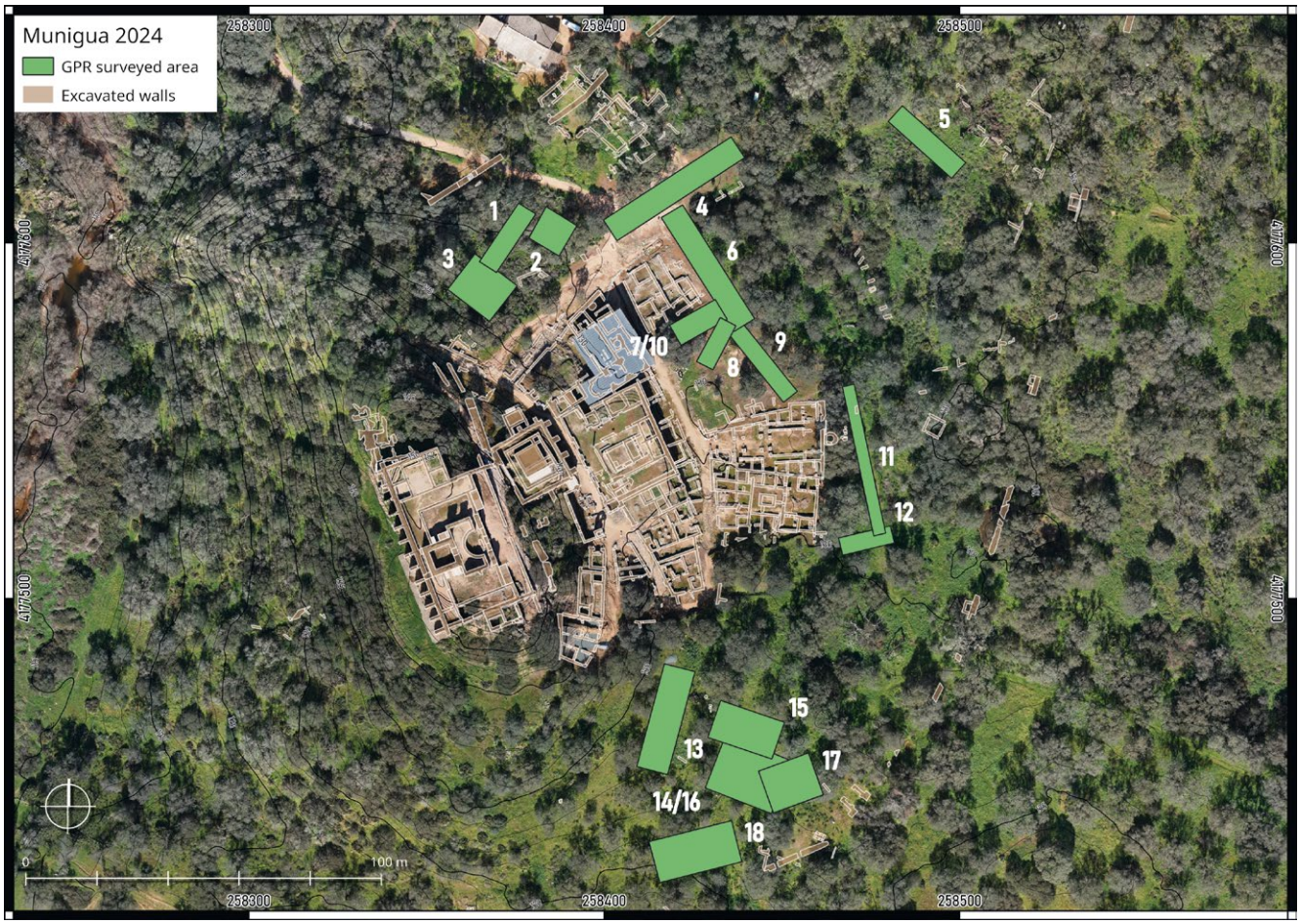

1

Fig. 1: Plan of Munigua with visible structures and grids surveyed.

2 Methodology and Surveyed Areas

7 Between August 25 and September 5 2024, a systematic ground-penetrating radar (GPR) survey was conducted at the Munigua/Mulva archaeological park[13]. A total of 18 survey grids (2.774 m^2) of varying sizes were examined (Fig. 2). The collected data was expected to provide detailed insights into subsurface structures[14], supporting a more comprehensive understanding of Munigua's spatial organization, and long-term occupation history.

8 The selection of survey grids was strategically planned to balance archaeological relevance, accessibility, and feasibility. Given the steep slopes, rocky formations, and dense vegetation present across the site, a targeted approach was necessary. The areas chosen for survey were those where surface clearance was possible, allowing efficient data collection without excessive resource expenditure. Although a broader survey would have been beneficial, limitations in logistics and environmental conditions required focusing on high-priority zones, particularly areas with promising archaeological potential or limited previous exploration.

9 For the survey, a GSSI Utility Scan antenna system with a frequency of 350 MHz was used, paired with an Emlid RS+ DGPS system operating in a rover-base

13 Apart from the authors, participants in this campaign were Axel Miß, Damaris Axmann and Joel Linares whom we would like to thank for their help. The GPR was generously lent by the Institute of Prehistory of the Friedrich-Alexander-Universität Erlangen-Nürnberg. We would like to thank Prof. Thorsten Uthmeier, Prof. Doris Mischka and Dr. Carsten Mischka.

14 Goodman – Piro 2013, 1 f.; Manataki et al. 2015, 13 f.

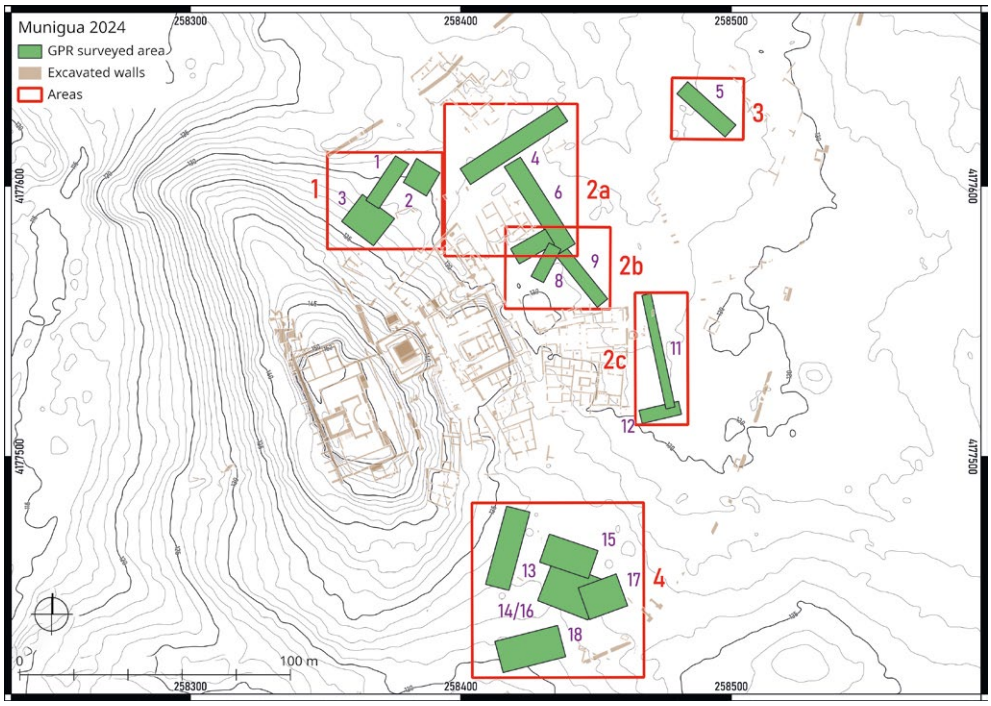

Fig. 2: Plan of Munigua with visible structures (brown), areas described in the text (red) and grids surveyed (green). Base map: iph Huelva, DAI Madrid.

2

configuration[15]. The use of mobile devices for data synchronization allowed for real-time positional accuracy, ensuring that the surveyed grids were properly aligned with previously mapped archaeological features.

10 The survey was conducted by marking each grid with fixed reference points, followed by systematic data collection along parallel lines at 0.25 m intervals. This high-density grid design was chosen to detect even small-scale subsurface anomalies, maximizing the resolution of the recorded reflections. Measurement lines were adjusted based on topographical features, allowing researchers to navigate around obstacles such as trees, rock formations, and excavation debris while maintaining continuous and precise coverage of the designated areas. These prerequisites resulted in different orientations of walking to maximize efficiency. To improve the accuracy of structural interpretations, two grids (Grid 7/10 and Grid 14/16) were surveyed twice in perpendicular directions. This methodological step aimed to determine whether data collection from multiple angles could enhance visibility or reveal additional structural details.

11 Once data collection was complete, processing was carried out using REFLEX3DScan software (Sandmeier Geophysical Research). The raw radar data underwent a series of four key processing steps to refine clarity and improve interpretability:

1. Start-time correction – Adjusting the signal timing to improve depth calibration.
2. Bandpass Butterworth filter – Removing unwanted frequency noise to enhance signal clarity.
3. Gain adjustment – Amplifying weaker reflections, making subtle subsurface features more visible.
4. Background removal – Eliminating large-scale noise interference, allowing smaller architectural anomalies to stand out.

12 The processed data was then assembled into a three-dimensional data cube, allowing for the visualization and extraction of individual time slices. The actual depth

15 Munigua is situated between higher hills, which occasionally affected GNSS measurements due to inconsistent satellite reception. On some days, signal quality was reduced, resulting in a measurement error of approximately 0.10 m.

of these slices was determined using the pre-set dielectric constant, which in Munigua consistently ranged between 12 and 16[16]. This ensured depth estimates remained accurate and consistent across different grids. The survey grids were distributed across four distinct areas and the results are as follows:

3 Results

13 The results of the GPR survey are displayed in grayscale images, where anomalies appear as deviations from the calibrated baseline values established on-site. These anomalies take various geometric forms, including circles, squares, and rectangular structures. Linear and rectangular features are typically interpreted as potential walls or architectural remains, as their orientation and dimensions often correlate with known structural patterns. The visibility of these features varies with depth, with some becoming less distinct as the depth increases, while others remain clearly identifiable[17].

Area 1 (Fig. 3)

14 Area 1 (Grids 1–3) is located between the bath complex and the northern city wall, extending southwest toward the terraced sanctuary. This area is partially enclosed by trees and excavation debris, likely remnants of previous archaeological investigations. Grids 1 and 2 were positioned on relatively flat ground, facilitating smooth GPR data collection. Grid 3, however, extended onto a sloping section, requiring adjustments in measurement protocols to account for terrain variations and ensure accurate depth readings[18].

15 Grid 1 measures 5.7 m × 20.0 m. In the upper 0.5 m[19], an anomaly appears in the northeast, consisting of a structure running northwest to southeast. In the middle of this feature, a 3.0 m long structure extends at a right angle to the southwest. It bends again at a right angle towards the southeastern boundary, forming an L-shape. Near the southeastern boundary, a nearly square structure measuring 2.0 m × 2.0 m appears in the centre of the southern half. The square structure is connected with the L-shape by a 4.0 m long structure. On the northwestern edge, a triangular feature measuring 4.0 m × 2.0 m is visible, positioned opposite the square feature. Several smaller anomalies are present in the southern third of the grid but do not appear to extend into deeper layers. There are no clearly recognizable structures visible beyond a depth of 0.5 m.

16 Grid 2 measures 10.0 m × 10.0 m and is located 1.5 m east of Grid 1. Anomalies along the southeastern edge correspond to backfill material, forming an irregular segment measuring approximately 4.0 m long and extending 2.0 m into the grid. Features are visible down to a depth of 0.5 m. Approximately 1.5 m west of the eastern corner, a 0.5 m wide linear structure runs north to south. Another parallel strip is visible 2.5 m to the west, forming two closely aligned linear anomalies. From the middle of the second structure, an L-shape is connected perpendicularly.

17 Grid 3 measures 13.0 m × 15.0 m and is directly south of Grid 1. Features remain visible down to a 0.5 m depth. At the southern end, a 7.0 m long, 1.0 m wide strip

16 At the time of the GPR survey, there had been no rainfall for several months, resulting in extremely dry soil conditions.

17 All measurements should be considered approximate, as the features do not always appear as clearly defined linear structures.

18 Further methods in postprocessing regarding the calculation of slope and GPR data processing, cf. Goodman et al. 2006; Goodman – Piro 2013, 119–127.

19 In this article ›upper‹, ›lower‹ and ›depth‹ measurements are in accordance to the depth slices from the results. Also, most of the structures noticed can be measured as about 0.5 m wide. If there is no considerable deviation from this, it will not be mentioned.

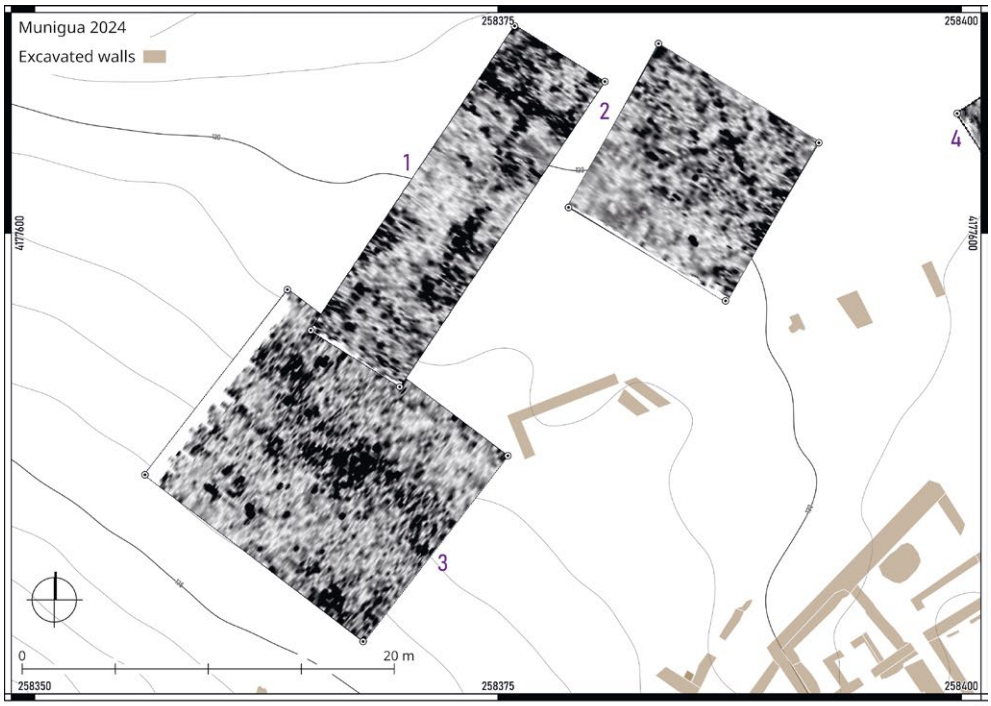

Fig. 3: Area 1 with single timeslices around 0.4 m depth (top) and highlighted features in the grayscale image (bottom). (Grid 1: 8.0349 ns, 0.40175 m; Grid 2: 7.4285 ns, 0.37143 m; Grid 3: 7.8833 ns, 0.39417 m.).

3

runs east to west. At its eastern end, a 5.0 m long, north-south oriented structure intersects, although its eastern edge appears less distinct. At the northern end of this structure, another 5.0 m long strip extends westward, running parallel to the southern anomaly. In the centre of the grid, a broad, flat anomaly measuring 4.0 m × 2.0 m appears, contributing to the unclear boundary of the northernmost structure. To the west of this anomaly, a north-south oriented strip measuring 8.0 m in length emerges. At its northern end, 3.0 m south of the northern grid boundary, a final, 5.0 m long strip extends east-west. Deeper anomalies at a 0.6–0.8 m depth consist mostly of small, rounded features appearing at regular intervals, loosely following the east-west orientation of the larger structures.

18 The anomalies detected in Area 1 show two distinct orientations, suggesting that they correspond to different building phases or architectural alignments. The features in Grid 1 appear to follow the orientation of the retaining walls on the slope to the south, the eastern boundary walls of the baths, and the western boundary of the bath complex. In contrast, the features in Grids 2 and 3 align more closely with walls north of the modern path leading to the terraced sanctuary (trenches 445 and 446), as well as with internal structural elements of the baths and adjacent residential buildings[20]. The difference in orientations between the anomalies could suggest that this area underwent multiple construction phases or different functional zones intersected here.

19 The retaining walls southwest of Grid 3 were dated to the Flavian period, while the thermal complex was dated to the late Julio-Claudian era[21]. The pathway up to the sanctuary, so-called Calle de la Ladera, could only vaguely be dated in use to the 1st to 4th centuries CE[22]. If it was already in use by the 1st century, there could be an argument for an earlier dating for this orientation[23]. The trenches 445 and 446 were dated to the Severan period and later and are the closest parallels in terms of orientation and space[24]. Unfortunately, very little is known about these excavations, but this orientation could potentially be later than the one in Grid 1.

20 Despite these observations, the surveyed sections remain too small to determine their exact function with certainty.

Area 2 (Fig. 4. 5. 6)

21 Area 2 (Grids 4. 6–12) lies on a levelled section east of existing excavation trenches. It is bordered by trees to the east and excavation areas to the west, forming a relatively enclosed but accessible space. Grid 6 was affected by a tree in the northwestern corner, which caused localized interference in the data. In Grids 7/10–9, backfill deposits from earlier excavations intruded into the surveyed area, potentially influencing the interpretation of subsurface features. Grids 11 and 12 followed modern footpaths, making them easier to access.

22 Grid 4 measures 7.0 m × 43.0 m. Features were clearly visible down to 0.9 m. Two parallel structures appear in the northeastern section, running from northwest to southeast. The eastern structure is 2.0 m wide, while the western one is 0.6 m wide. To the west of these two features, a rectangular structure is evident, which remains open in the southwest. In the southwestern part of the grid, several isolated, elongated structures can be seen. These do not appear to be directly connected to each other but share the same general orientation.

23 Grid 6 measures 7.0 m × 38.0 m and is south of grid 4. Features could be clearly recognized down to a depth of 0.5 m. In the southern part, three parallel, elongated structures run in a southwest to northeast direction. The eastern extent of these structures cannot be determined, as they continue beyond the grid boundary. North of these three parallel strips, a larger anomaly spans the entire width of the grid, running from northeast to southwest and measuring 1.5 m wide. A 3.0 m wide strip extends northward from this structure, ending after 4.0 m. Further north, a similar feature can be seen. In the

20 Schattner 1999, 49.

21 Schattner 2019, 123 f.: the main indication for the typological comparisons and metallurgical furnaces dated to before the middle of the 1st century CE.

22 Calle de la Ladera: Schattner 2003, 77.

23 The presence of regularly spaced, smaller anomalies at deeper levels may indicate pavement remains, postholes, or smaller architectural features.

24 Schattner 1999, 49. – Also, House 5 has a similar orientation and is dated to the second half of the 1st century CE in its first phase (Schattner 2019, 146). But as it is relatively far away and was inhabited into the 3rd century CE there is no real hint here.

Fig. 4: Area 2a with single timeslices around 0.4 m depth (top) and highlighted features in the grayscale image (bottom). (Grid 4: 7.7317 ns, 0.38659 m; Grid 6: 7.4285 ns, 0.37143 m).

4

northeastern part of the grid, another anomaly runs from northeast to southwest. At its western end, this structure has two extensions, branching north and south.

24 Grid 7/10, measuring 6.5 m × 15.0 m, was surveyed twice. In both orientations, similar features remained visible down to 0.5 m, which leads to a combined description as one grid[25]. In the southwestern part, two parallel, elongated structures, each 1.0 m wide, run from north to south. The longer structure along the southeastern edge of the grid is not fully captured within the grid, making its exact dimensions uncertain.

25 In Grid 10 new anomalies became visible from a depth of 0.8 m, fading at 1.0 m.

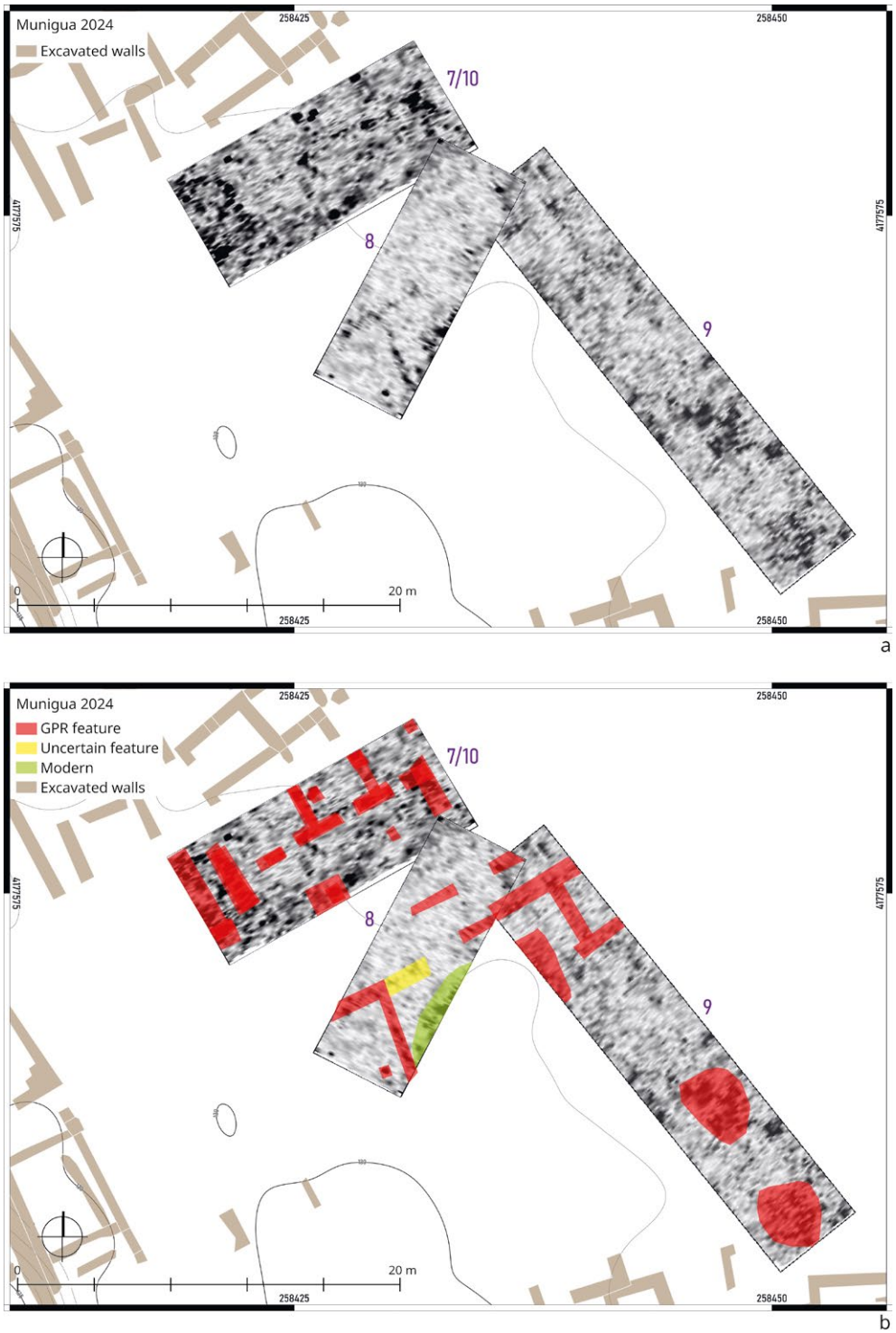

5

Fig. 5: Area 2b with single timeslices around 0.4 m depth (top) and highlighted features in the grayscale image (bottom). (Grid 7/10: 6.0641 ns, 0.3032 m; Grid 8: 8.9445 ns, 0.44723 m; Grid 9: 7.1253 ns, 0.35627 m).

An elongated feature runs diagonally across the grid from west to east, with three interruptions creating four distinct segments. The westernmost segment measures 0.6 m in width and 1.5 m in length. Two T-shaped structures follow. The easternmost segment is 1.7 m long and has a 2.0 m long extension at its eastern end. In the southeastern part of the grid, a rectangular structure is present.

25 Grid 8 measures 6.0 m × 15.0 m. Anomalies were clearly visible down to a depth of 0.7 m. In the southwestern part, a rectangular structure is present, with one segment oriented east-west before bending at a right angle to the south. The endpoints of this feature extend beyond the grid boundary. In the northwestern part, three smaller

Fig. 6: Area 2c with single timeslices around 0.25 m depth (top) and highlighted features in the grayscale image (bottom). (Grid 11: 5.0078 ns, 0.25039 m; Grid 12: 5.0078 ns, 0.25039 m).

6

parallel structures were identified, sharing the orientation of the larger southwestern structure. Two of them extend beyond the grid boundary.

26 Grid 9 measures 5.0 m × 26.0 m. Features were visible down to a depth of 0.8 m. Two large structures dominate the northern section. One is a rectangular feature – almost an H-shape – that extends beyond the grid boundary to the northeast and southwest. Adjacent to this structure on the west is a trapezoidal anomaly that tapers towards the south. In the southeastern section of the grid, two anomalies without clearly defined shapes are present.

27 Grid 11, measures 3.5 m × 43.0 m. Due to the extensive and irregular distribution of anomalies, no clearly identifiable archaeological features were detected.

28 Grid 12, measures 5.0 m × 15.0 m. Features were visible down to a depth of 1.0 m. In the western part, an elongated feature was detected, wider in the north and tapering southward, though it was cut off by the grid boundaries. At the centre of the grid, an L-shaped structure appears. In the eastern section, a north-south oriented structure runs through the grid. At a depth of 0.25 m, another slightly rotated strip measuring 0.8 m wide runs parallel to it.

29 The GPR survey in Area 2 revealed a significant number of structural anomalies that exhibit characteristics indicative of walls and architectural remains. Nearly all detected anomalies correspond to the direction of existing walls, confirming their architectural nature. The depth of these features matches the preserved walls in excavation sections, particularly in Grid 7/10, where structures on the northern edge correspond to known architectural elements in house 5 (trench 230)[26]. The anomalies in the eastern part of Grid 4 correspond very well to the walls excavated southeast of the grid in trench 238, which are dated to the Severan and later periods[27]. The excavated structures of the grid are slightly changed in orientation compared to the GPR features[28].

30 Several walls extend across multiple grids, such as a northwest-southeast oriented feature spanning from Grid 7/10 into Grid 6 and a rectangular structure in Grid 9 continuing westward into Grid 8. The proximity of the surveyed Grids 6–10 to previously excavated Houses 1 and 5 provides a chronological reference, as these structures date between the late 1st and early 3rd centuries CE[29].

31 Grids 11 and 12 are situated along modern paths. The anomalies in these grids may result from modern disturbances rather than archaeological remains. However, the possibility of underlying archaeological structures obscured by later disturbances cannot be entirely ruled out.

Area 3 (Fig. 7)

32 Area 3 (Grid 5) is situated east of the terraced sanctuary, within the necropolis sector. The grid is surrounded by dense tree cover, limiting the available survey space. Located more than 40 m from the nearest residential buildings, this sector provided an opportunity to explore burial practices and spatial organization within the necropolis. The presence of thick undergrowth posed challenges, but the surveyable area was expanded, yielding a broader and more informative dataset.

33 Grid 5 measures 6.0 m × 24.0 m. Within this grid, two distinct structural anomalies were identified, both of which are visible at varying depths. In the southeastern part of the grid, an almost square structure is evident, measuring approximately 2.5 m on each side. The structure is clearly defined at depths between 0.4 and 0.9 m. In the central part of the grid, an L-shaped structure was identified, distinguishable between depths of 0.3 and 0.6 m. The northwest-southeast segment measures 6.0 m in length, while the perpendicular segment, also running northwest to southeast, extends 3.2 m.

26 Schattner 2019, 146.

27 Cf. Schattner 2022, 244 fig. 3.

28 Also, not much is known here about the excavation results, other than their dating to the Flavian period (Schattner 2022, 244 fig. 3).

29 Meyer 2001, 41 f. 90; Schattner 2019, 146. Also, the western part of Grid 4 aligns well with walls of House 5. The loosely defined anomaly in the southern part of Grid 9 could be connected to the orientation of the northern walls of House 1.

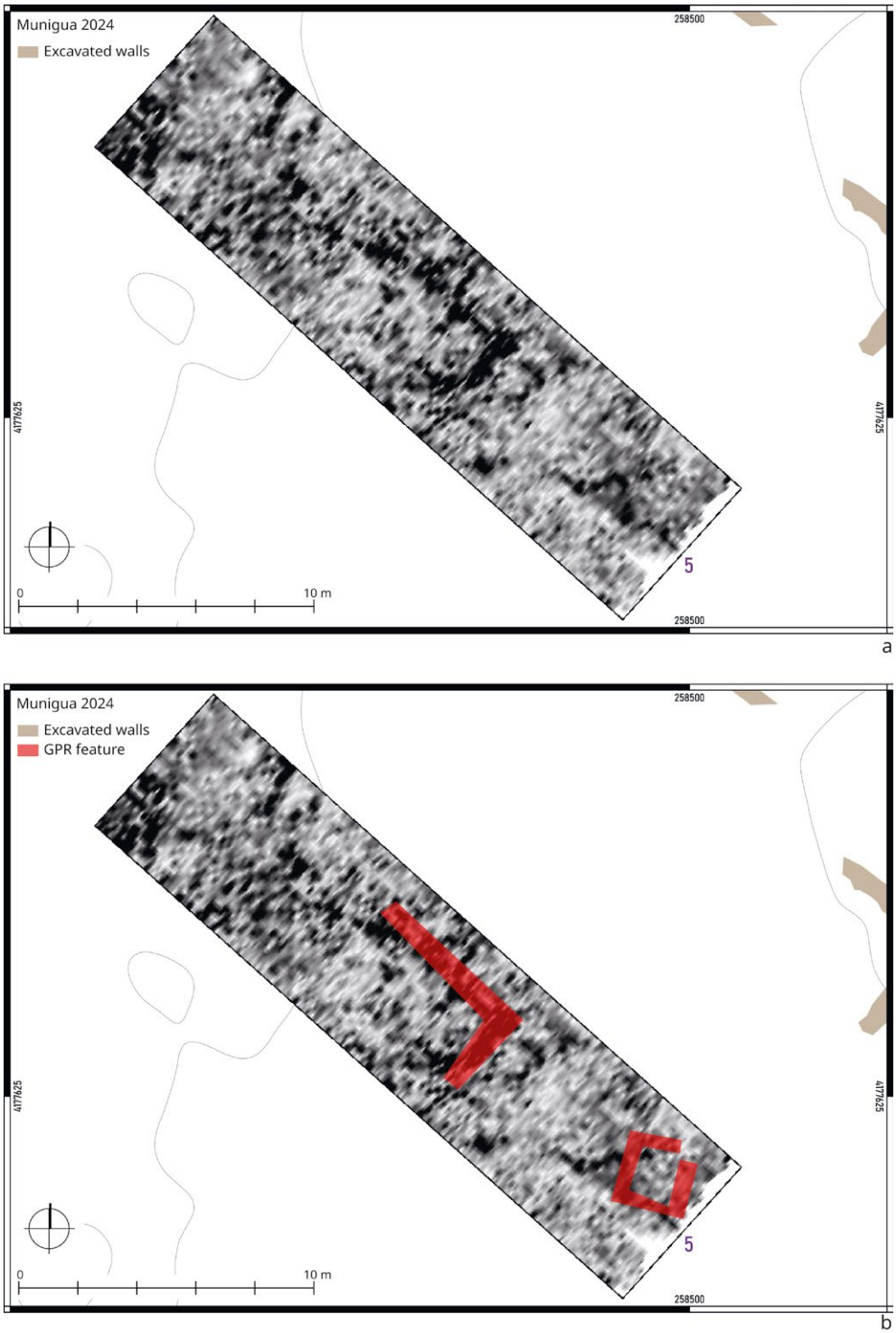

Fig. 7: Area 3 with single timeslices around 0.4 m depth (top) and highlighted features in the grayscale image (bottom). (Grid 5: 8.0349 ns, 0.40175 m).

7

34 Area 3 is closest to the excavated eastern necropolis of Munigua[30]. Only a small area of trenches, dug in 1957–1958, reveals parts of a system of walls surrounding groups of graves, present also at the southern necropolis[31]. These enclosures walls are

30 Raddatz 1973; Blech et al. 1993.

31 For the ›Ostnekropole‹ cf. Raddatz 1973, 18–20 plan 2–4; Kobusch 2014, 248 f. – For the ›Südnekropole‹ cf. Vegas 1988, 10 f. suppl. 6; Kobusch 2014, 247 f. – Previous excavations near the grid did partially reveal walls. While trench 417 was a continuation of the eastern necropolis, trench 419 was beneath Grid 5 and, apparently, did not reveal any structures (Schattner 2000, 74). – For a general discussion of burial enclosures in Roman Spain cf. Kobusch 2014, 85–101.

structural divisions within the cemetery area, which could be related to the features detected in the current survey.

35 The graves were dated to the Imperial to late Antique period, specifically from the 2nd to 4th century CE[32]. The identified L-shaped structure could be an enclosure wall, which aligns loosely with the surrounding architectural features of the necropolis. The square feature could be a grave, similar to different examples in the necropolis[33]. However, due to the limited extent of the surveyed area, it is not possible to confidently assign these structures to any specific burial type observed within the cemetery[34].

36 Expanding the geophysical survey to adjacent sections of the necropolis or conducting targeted excavations could clarify the function of these anomalies and provide more detailed insights into the burial practices and spatial organization of the cemetery.

Area 4 (Fig. 8. 9)

37 Area 4 (Grids 13–18) extends southeast of the terraced sanctuary, reaching the vicinity of the city wall. This area features a gradual north-to-south slope, which influenced GPR data interpretation. Many grids in this section were framed by tree lines, requiring careful alignment to minimize signal disruption[35].

38 Grid 13 measures 9.0 m × 30.0 m. No structures were detected below a depth of 1.35 m and the features in this grid were faintly visible. The most prominent anomaly is a flat feature located at the southern end. It is most visible between 0.9 and 1.3 m in depth. A right-angled structure follows 0.5 m to the north, beginning at the western corner of the flat anomaly. This consists of a 2.0 m long strip running southeast to northwest, which then extends at a right angle to the northeast for a further 3.0 m. The feature continues in a zig-zag pattern towards the east. The northern half of the grid contains only two flat anomalies located along the northwestern edge.

39 Grid 14/16, measuring 16.0 m × 20.0 m, was surveyed twice in different directions. Features are generally more pronounced in Grid 16 than in Grid 14, leading to their combined description as a single unit. Interpretable anomalies are visible to a depth of 0.9 m. In the northern part, elongated rectangular anomalies aligned east-west were detected between depths to 0.4 m. These form three adjacent rectangular features of varying sizes with a total length of 12.5 m and maximum width of 4.5 m. The central rectangle contains an internal square feature measuring 1.5 m × 1.5 m. Beyond this depth, a right-angled square with sides of 1.7 m remains distinguishable, but no further structures are identifiable below this level.

40 Grid 15 measures 15.0 m × 19.0 m. Its southern portion overlaps with the northern part of Grid 14/16. The rectangular structure identified in Grid 14/16 remains visible in the southern corner of Grid 15 down to 0.9 m in depth. At the northeastern edge, up to a depth of 0.6 m, a 3.0 m wide strip appears, extending east-west from the eastern boundary to the northwestern corner. Directly south of this, a narrow parallel strip is present.

41 Grid 17, measures 12.5 m × 15.0 m, with its western portion overlapping the eastern part of Grid 14/16. A flat anomaly measuring 1.5 m in diameter, likely related to the remains and roots of a palm tree, was identified in the centre of the grid. Structures are visible in the upper 0.6 m. A flat anomaly extends from the northern corner. Another flat anomaly is visible in the eastern corner. A strip extends from the northeastern

32 Raddatz 1973, 39–41; Kobusch 2014, 248.

33 e. g. ›Ostnekropole‹, suppl. 11 (Raddatz 1973, 57–59) or ›Südnekropole‹, Grab 60 (Vegas 1988, 84).

34 Vegas 1988, Beil. 6. – For the most common burial types in Roman Spain cf. Kobusch 2014, 15–114.

35 A notable feature in this area is a semi-circular depression in Grid 14/16. This depression was likely formed due to stone extraction activities in the 1950s. Further investigation will be necessary to determine whether this feature is of natural origin or an archaeological structure.

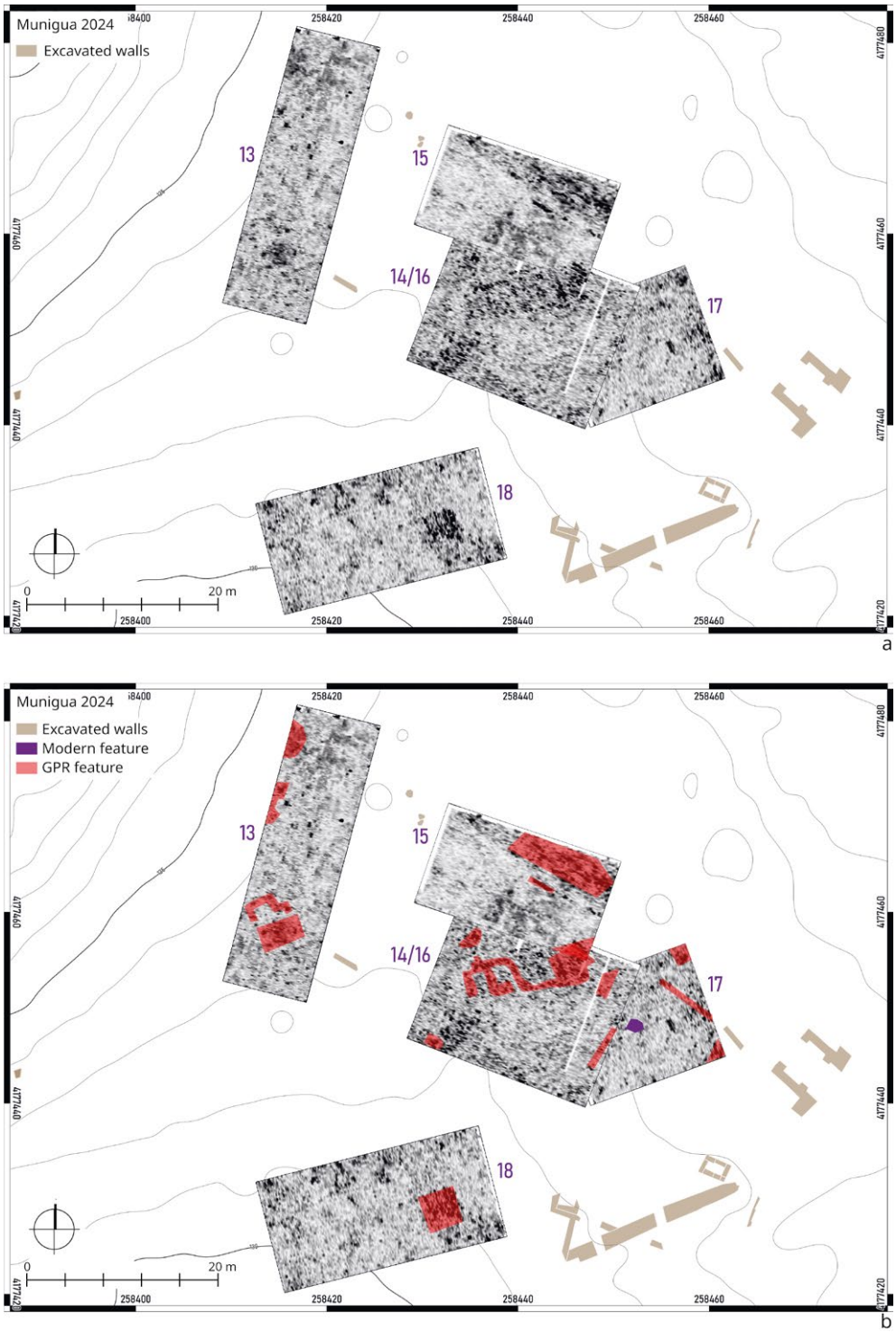

Fig. 8: Area 4 with single timeslices from different depth (top) and highlighted features in the grayscale image (bottom). (Grid 13: 22.379 ns, 1.1189 m; Grid 14/16: 6.5727 ns, 0.32864 m; Grid 15: 12.520 ns, 0.6259 m; Grid 17: 6.1033 ns, 0.30516 m; Grid 18: 7.0522 ns, 0.35211 m).

8

boundary into the grid for 7.5 m in a northwestern direction. In the southern part, another strip measuring 6.0 m runs southwest to northeast.

42 Grid 18, measuring 12.0 m × 24.0 m. No clear structures are discernible below 0.5 m. A square anomaly measuring 3.5 m per side appears in the centre of the eastern half.

43 The overall results from Area 4 suggest that structural remains are difficult to distinguish, with some anomalies appearing more loosely defined than expected. The comparison with data from the 2015 survey indicates that, while the area contains

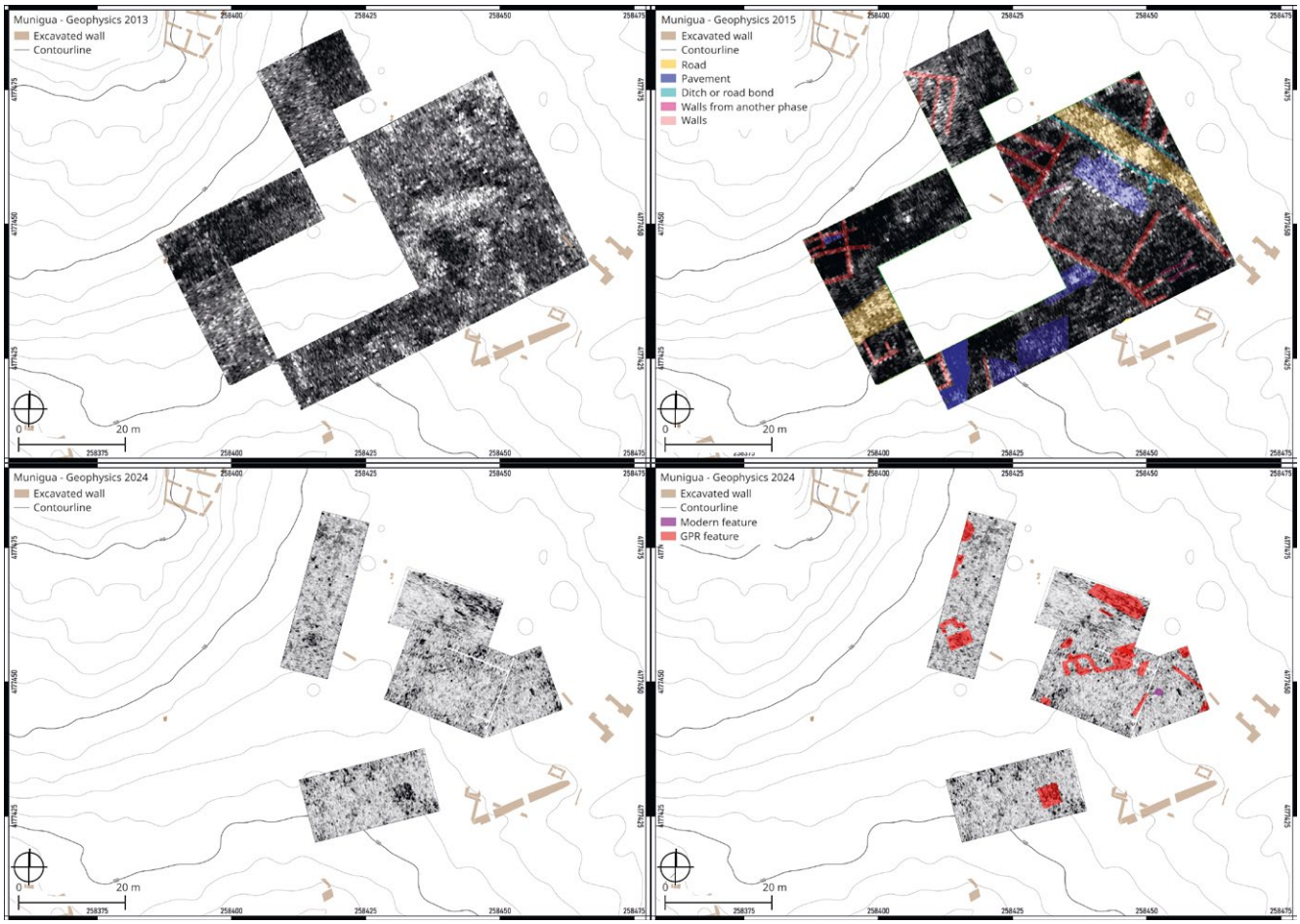

9

Fig. 9: Comparison of the GPR results from 2015 (top) and 2024 (bottom) on similar timeslices. Top left: Timeslice 0.36–0.63 m. – Top right: Timeslice 0.63–0.77 m. – Bottom: cf. fig. 7.

dispersed features, their clarity and consistency vary significantly[36]. By refining the resolution through a denser scan grid, new details were detected, particularly regarding connections between previously known structures. The alignment of features in the northern parts of Grid 15 and Grid 17 suggests a possible extension towards the already excavated gate[37], raising the possibility that this could be part of a street pavement extending westward before turning northwards east of Grid 13. This route may have continued toward the road leading to the forum[38]. The three-room structure in the norther part of Grid 14/16 was partially visible on the surface, but did not show up in the earlier survey. However, the 20.0 m × 20.0 m large structure detected in 2015 (Fig. 9) could not be seen in the results of the present survey[39]. One reason for the different results could be the frequency of the antennas and differences in soil texture together with different distance between lines.

44 A new excavation, started directly after the GPR survey, confirmed that the earlier Roman structure was a large and significant architectural feature, likely part of the broader urban development of Munigua during antiquity[40]. The divergence in

36 Schattner et al. 2017, 140–142.

37 Cf. Vegas 1988, suppl. 1: trenches 221–224 are the gate and the surrounding area inside the walls. Unfortunately, not much is known about the dating of this gate (Schattner 2019, 161 fig. 4.90).

38 Schattner et al. 2017, 142.

39 The long features in Grid 17 align with features from the 2015 survey. Even the northern anomaly from Grid 13 and the single anomaly in Grid 18 loosely match previously interpreted features Schattner et al. 2017, 142 fig. 20.

40 The excavation will be published by the excavators Alexander Hoer and Axel Miß in a future paper.

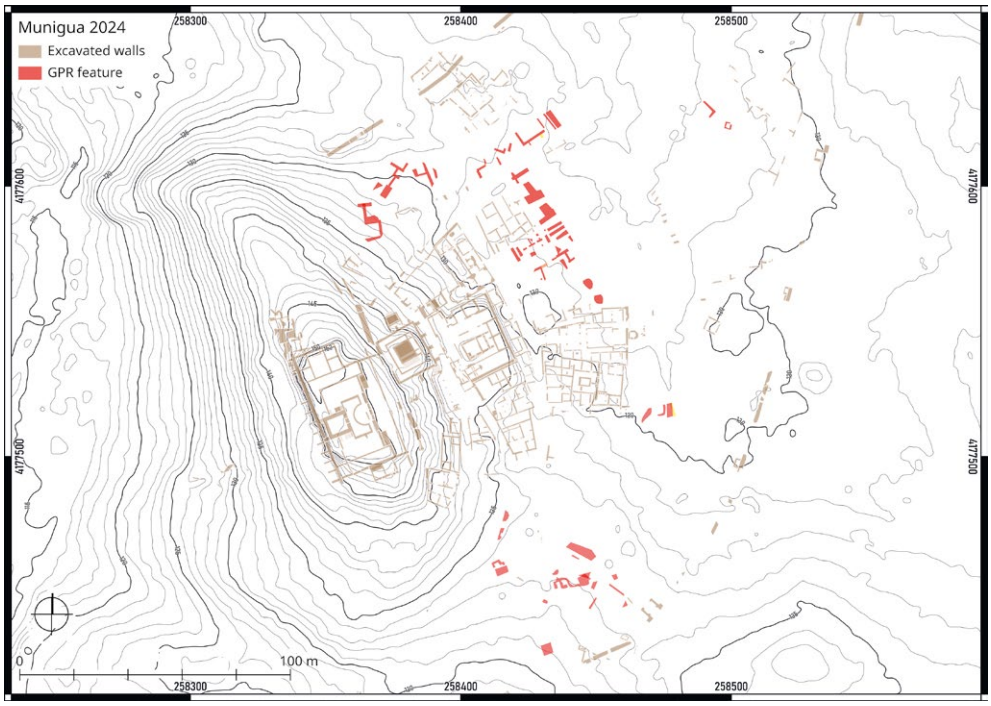

Fig. 10: Plan of Munigua with visible structures (brown) and newly found GPR features (red).

10

orientation and the differences in stratigraphy suggest a clear sequence of reuse and modification, demonstrating how this part of the site was repurposed over time, transitioning from a major Roman building to an early medieval settlement phase[41]. These findings highlight the long-term continuity and transformation of urban space in Munigua across different historical periods.

4 Conclusions (Fig. 10. 11)

45 The 2024 GPR campaign at Munigua has substantially improved our understanding of the site's spatial organization and diachronic development. By targeting key areas across the city – north and east of the bath complex, the eastern slope, the necropolis, and the southeastern zone near the city wall – the survey enabled the identification of previously undocumented features, clarification of structural sequences, and refinement of the city's extent.

46 In Area 1, north of the bath complex and south of the northern city wall, the survey recorded two clearly differing orientations of architectural remains. Anomalies in Grid 1 aligned with the eastern wall of the baths and the Flavian-period retaining walls, while features in Grids 2 and 3 followed the orientation of walls previously documented in trenches 445 and 446, as well as interior elements of the bath complex. The juxtaposition of these differing alignments points to multiple construction phases and possibly changing spatial organization over time. Their depth (c. 0.5 m) and geometry correspond well to known Roman wall constructions, although the limited survey area does not permit a definitive functional interpretation.

47 On the eastern slope (Area 2), the GPR results confirmed a dense architectural layout, particularly in Grids 4 and 6–10. Several anomalies aligned closely with structures known from previous excavations in the same sector, especially Houses 1 and 5, dated between the late 1st and early 3rd centuries CE. These findings point to the pres-

41 Teichner 1998.

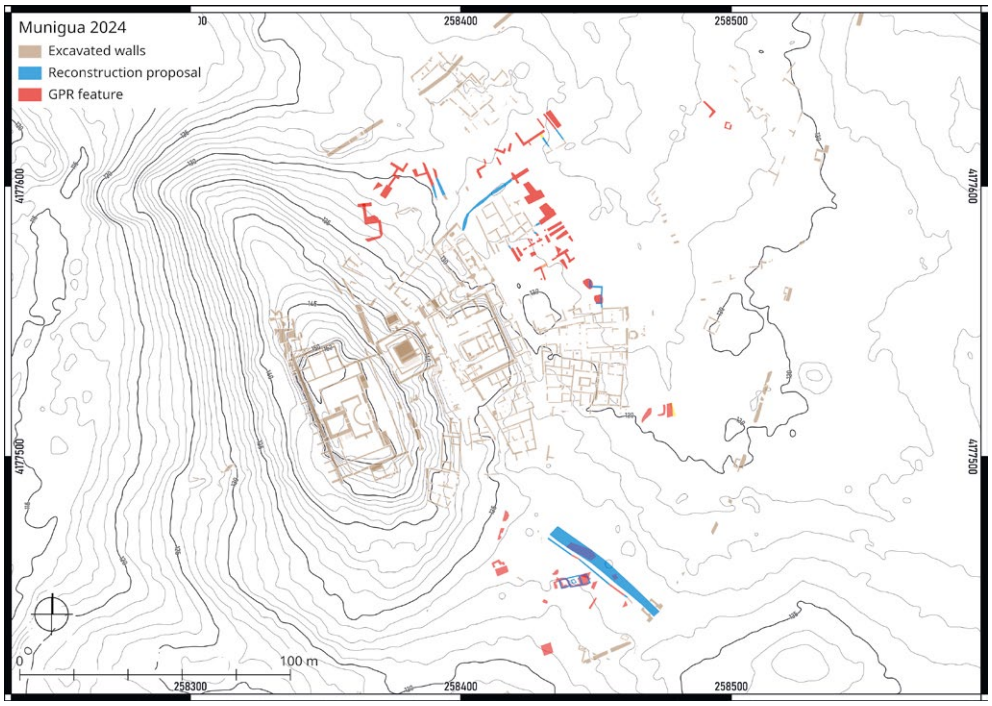

11

Fig. 11: Plan of Munigua with visible structures (brown) and newly found GPR features (red, yellow) and reconstructed connections to existing features (blue).

ence of large architectural units, likely domestic in character, extending across multiple grids. Grids 11 and 12, located along modern footpaths, yielded more ambiguous results. Certain anomalies – such as an L-shaped feature in Grid 12 – may indicate underlying structures, but the influence of modern surface disturbance must be considered.

48 In the necropolis sector east of the sanctuary (Area 3), Grid 5 revealed features resembling grave enclosures recorded during the 1957–1958 excavations and exhibit similar configurations to funerary precincts known from the eastern and southern necropolis. Based on parallels in form and location, and considering the 2nd to 4th century CE dating of previously excavated graves in this area, the newly identified features can tentatively be interpreted as part of the same funerary zone. However, due to the limited size of the survey area, their precise function and typology remain uncertain.

49 Area 4, southeast of the sanctuary and extending toward the city wall, produced particularly complex results. In Grids 14/16 and 15, rectangular and L-shaped anomalies were identified, forming a compact structure visible down to 0.9 m depth. Notably, these features exhibit a different orientation from deeper anomalies in the same area. The deeper structure – measuring approximately 20.0 m × 20.0 m – had already been detected during the 2015 survey, but the higher-resolution scan from 2024 allowed for better delineation of the upper layers. The differing alignments strongly suggest a reorganization of the area, with multiple phases of construction. Excavations initiated immediately after the survey confirmed the presence of a later building constructed above the Roman structure, possibly dating to the early Islamic period, though the final interpretation is pending and will be published separately. At present, the GPR data indicate only potential phases of the structures, not their absolute dating.

50 Additional anomalies recorded in Grids 13, 17, and 18 may indicate paved surfaces or street segments, with several linear features in Grids 15 and 17 aligning with the trajectory of the known northern gate and road toward the forum.

51 Overall, the 2024 data expand the known footprint of Munigua. In the northern sector, newly documented features extend the slope-parallel alignment of excavated structures and support long-standing assumptions about dense urban development in this area. In the northeast, additional anomalies include both continuations of known

architectural lines and deviations suggesting later reuse or transformation. These findings reflect the dynamic evolution of the site, including the reconfiguration of spaces across the Roman and Late Antique periods.

52 From a methodological standpoint, the 2024 campaign employed a denser scan grid (0.25 m spacing), which allowed for the improved detection of narrow features such as wall lines. However, this higher resolution detected anomalies at a greater depth – such as those identified in the 2015 survey – less visible. Most features were detected at a 0.3–0.5 m depth, whereas deeper anomalies previously recorded below 0.6 m were largely absent in 2024. While earlier experiments with geoelectrical and geomagnetic prospection yielded mixed results due to soil conductivity and slag content, GPR once again proved to be the most effective method under the site's geological conditions.

53 In sum, the 2024 GPR campaign clarified architectural sequences, extended the known spatial limits of the city, and revealed new evidence for post-Roman use of the urban space. The identification of a building constructed above a large Roman structure in Area 4 represents the first architectural indicator of early medieval activity at the site. When considered alongside prior excavations and earlier surveys, the 2024 results contribute significantly to a more nuanced reconstruction of Munigua's long-term development and underscore the role of high-resolution, non-invasive geophysics as a central tool in archaeological research at complex, multi-phase sites.

54 Further geophysical investigation within Munigua's urban area is highly desirable, especially in zones that remain unexamined or only partially covered. However, extensive vegetation currently limits ground-based survey work and would require significant effort and cost for clearing. In this context, emerging applications of airborne or drone-mounted GPR systems may offer a promising and more economical alternative for future investigations[42]. Such methods could enable broader coverage without invasive terrain preparation and thus open new possibilities for continued exploration of Munigua's spatial and historical dynamics.

42 For example Frid – Frid 2024.

References

Blech et al. 1993 M. Blech – Th. Hauschild – D. Hertel, Mulva III. Das Grabgebäude in der Nekropole Ost. Die Skulpturen. Die Terrakotten, MB 21 (Mainz 1993)

Coarelli 1987 F. Coarelli, Munigua, Praeneste e Tibur. I modelli laziali di un munivipio della Baetica, Lucentum 6, 1987, 91–100

Frid – Frid 2024 M. Frid – V. Frid, A Case Study of the Integration of Ground-Based and Drone-Based Ground-Penetrating Radar (GPR) for an Archaeological Survey in Hulata (Israel). Advancements, Challenges, and Applications, Applied Sciences 14 (10), 2024, 4280

Goodman – Piro 2013 D. Goodman – S. Piro, GPR Remote Sensing in Archaeology, Geotechnologies and the Environment 9 (Berlin 2013)

Goodman et al. 2006 D. Goodman – Y. Nishimura – H. Hongo – N. Higashi, Correcting for Topography and the Tilt of Ground-Penetrating Radar Antennae, Archaeological Prospection 13, 2006, 157–161

Griepentrog 2008 M. Griepentrog, Mulva V. Die vormunizipale Besiedlung von Munigua, MB 29 (Wiesbaden 2008)

Kobusch 2010 P. Kobusch, Römische Grabbauten im Eingangsbereich hispanischer Städte, in: D. Vaquerizo Gil (ed.), Las áreas suburbanas en la ciudad histórica. Topografía, usos, función, Monografías de arqueología cordobesa. Nueva época 18 (Córdoba 2010) 117–134

Kobusch 2014 P. Kobusch, Die Grabbauten im römischen Hispanien. Zur kulturellen Prägung der Sepulkralarchitektur, Tübinger archäologische Forschungen 14 (Rahden/Westf. 2014)

Krug 2018 A. Krug, Mulva VI. Die Kleinfunde, MB 38 (Wiesbaden 2018)

Manataki et al. 2015 M. Manataki – A. Sarris – J. C. Donati – C. Ciemca Garcoa – T. Kalayci, GPR. Theory and Practice in Archaeological Prospection, in: A. Sarris (ed.), Best Practices of Geoinformatic Technologoices for the Mapping of Archaeolandscapes (Oxford 2015) 13–24

Meyer 2001 K. E. Meyer, Die Häuser 1 und 6, in: K. E. Meyer – C. Basas – F. Teichner (eds.), Mulva IV. Die Häuser 1 und 6. La cerámica de la casa N° 6. Das Haus 2, MB 27 (Mainz 2001)

Meyer et al. 2007 C. Meyer – B. Ullrich – Ch. D. M. Barlieb, Archaeological Questions and Geophysical Solutions. Ground-Penetrating Radar and Induced Polarization Investigations in Munigua, Spain, Archaeological Prospection 14, 2007, 202–212

Raddatz 1973 K. Raddatz, Mulva 1. Die Grabungen in der Nekropole in den Jahren 1957 und 1958, MB 2 (Mainz 1973)

Schattner 1999 Th. G. Schattner, Sucinto informe de las excavaciones arqueológicas en Munigua 1999, AnArqAnd 1999/II, 47–52

Schattner 2000 Th. G. Schattner, Sucinto informe de las excavaciones arqueológicas en Munigua 1998, AnArqAnd, 2000/II, 70–75

Schattner 2003 Th. G. Schattner, Munigua. Cuarenta años de investigaciones, Collección Arqueología (Serie Monografías) 16 (Seville 2003)

Schattner 2004 Th. G. Schattner, Gedanken zu Situation und Lage des Terrassenheiligtums von Munigua (Prov. Sevilla), in: E.-L. Schwandner – K. Rheidt (ed.), Macht der Architektur – Architektur der Macht. Bauforschungskolloquium in Berlin vom 30. Oktober bis 2. November 2002 veranstaltet vom Architektur-Referat des DAI, DiskAB 8 (Mainz 2004) 241–249

Schattner 2007 Th. G. Schattner, El inicio de las investigaciones en Munigua, in: M. Belén Deamos – J. Beltrán Fortes (eds.), Las instituciones en el origen y desarrollo de la arqueología en España, Spal Monografías 10 (Sevilla 2007) 43–66

Schattner 2019 Th. G. Schattner, Munigua. Un recorrido por la arqueología del ›Municipium Flavium Muniguense‹ (Sevilla 2019)

Schattner 2022 Th. Schattner, Munigua, in: T. Nogales Basarrate (ed.), Ciudades romanas de Hispania II, Hispania Antigua (Serie Arqueológica) 14 (Rome 2022) 241–252

Schattner in press Th. Schattner (ed.), Mulva VIII. Die wirtschaftlichen Grundlagen, MB 43 (in press)

Schattner et al. 2017 Th. G. Schattner – A. Azcárraga Cámara – K. Brose – B. Bouresh – M. Gutiérrez Rodriguez – A. Krug – W. Martini – H. Ruipérez – D. Schäffler – R. Scholz, Munigua, Spanien, e-Forschungsberichte 1, 2017, 128–142

Teichner 1998 F. Teichner, Spuren islamischer Besiedlung auf dem Castillo de Mulva (Villanueva del Río y Minas, prov. Sevilla)?, MM 39, 1998, 336–355

Vegas 1988 M. Vegas, Mulva 2. Die Südnekropole von Munigua. Grabungskampagnen 1977 bis 1988, MB 15 (Mainz 1988)

ZUSAMMENFASSUNG

Freilegung der verborgenen Stadtlandschaft von Munigua

Erkenntnisse aus dem Bodenradar-Survey 2024 und seine Implikationen für die römische und poströmische Besiedlung

Alexander Hoer – Fabian Gapp – Franziska Wanka

Die GPR-Kampagne 2024 in der römischen Stadt Munigua hat neue Baustrukturen dokumentiert, Bauabfolgen präzisiert und die bekannte räumliche Ausdehnung der Stadt erweitert. In vier ausgewählten Bereichen ermöglichten die hochauflösenden Messungen die Identifikation von Mauerresten, abweichenden Orientierungen sowie Umbauten von der römischen bis in die nachrömische Zeit. Besonders hervorzuheben ist ein Gebäude, das vermutlich in frühmittelalterlicher Zeit über einem älteren römischen Bau errichtet wurde – der erste architektonische Hinweis auf eine Nutzung des Ortes in dieser Epoche. Die Ergebnisse zeigen das große Potenzial geophysikalischer Methoden für die Erforschung komplexer, mehrphasiger Fundplätze.

SCHLAGWÖRTER

Römischer Städtebau, Munigua, Georadar, Nachrömische Transformation

RESUMEN

Desvelando el paisaje urbano oculto de Munigua

La prospección con radar de penetración terrestre de 2024 y sus implicaciones para la ocupación romana y posromana

Alexander Hoer – Fabian Gapp – Franziska Wanka

La prospección con georradar (GPR) realizada en 2024 en la ciudad romana de Munigua permitió identificar nuevas estructuras arquitectónicas, clarificar fases constructivas y ampliar el conocimiento sobre la extensión urbana del asentamiento. El estudio, llevado a cabo en cuatro sectores clave, reveló alineaciones murarias, variaciones en la organización espacial y transformaciones desde época romana hasta periodos posteriores. Entre los hallazgos más relevantes destaca una construcción reutilizada o modificada durante la Alta Edad Media, lo que representa el primer indicio arquitectónico de esa fase en el yacimiento. Los resultados confirman la eficacia del georradar en contextos arqueológicos complejos y enriquecen significativamente la comprensión de la evolución urbana de Munigua.

PALABRAS CLAVE

Urbanismo romano, Munigua, georradar, transformación posterior al periodo romano

ILLUSTRATION CREDITS

Titelbild: Authors: F. Gapp – F. Wanka, Copyright: DAI Madrid (image section)
Fig. 1: Authors: F. Gapp – F. Wanka, Copyright: DAI Madrid
Fig. 2: Authors: F. Gapp – F. Wanka, Copyright: DAI Madrid
Fig. 3: Authors: F. Gapp – F. Wanka, Copyright: DAI Madrid
Fig. 4: Authors: F. Gapp – F. Wanka, Copyright: DAI Madrid
Fig. 5: Authors: F. Gapp – F. Wanka, Copyright: DAI Madrid
Fig. 6: Authors: F. Gapp – F. Wanka, Copyright: DAI Madrid
Fig. 7: Authors: F. Gapp – F. Wanka, Copyright: DAI Madrid
Fig. 8: Authors: F. Gapp – F. Wanka, Copyright: DAI Madrid
Fig. 9: Top: after K. Brose and R. Scholz 2015, DAI Madrid: Bottom: authors: F. Gapp – F. Wanka, Copyright: DAI Madrid
Fig. 10: Authors: F. Gapp – F. Wanka, Copyright: DAI Madrid
Fig. 11: Authors: F. Gapp – F. Wanka, Copyright: DAI Madrid

CONTACT

Dr. Alexander Hoer
Deutsches Archäologisches Institut
Calle de Serrano 159
28002 Madrid
Spain
alexander.hoer@dainst.de
ORCID-iD: https://orcid.org/0009-0003-8410-1959

Fabian Gapp, M.A.
Universität Trier
Universitätsring 15
54296 Trier
Germany
s3fagapp@uni-trier.de
ORCID-iD: https://orcid.org/0009-0002-5832-8706

Franziska Wanka, M.A.
Friedrich-Alexander-Universität Erlangen-Nürnberg
Kochstraße 4/18
91054 Erlangen
Germany
franzi.wanka@fau.de
ORCID-iD: https://orcid.org/0009-0005-1525-7057

METADATA

Titel/*Title*: Freilegung der verborgenen Stadtlandschaft von Munigua. Erkenntnisse aus dem Bodenradar-Survey 2024 und seine Implikationen für die römische und poströmische Besiedlung/*Revealing the Hidden Urban Landscape of Munigua. Insights from the 2024 Ground-Penetrating Radar Survey and Its Implications for Roman and Post-Roman Occupation*
Band/Issue: MM 66, 2025
Bitte zitieren Sie diesen Beitrag folgenderweise/Please cite the article as follows: Alexander Hoer – Fabian Gapp – Franziska Wanka, Revealing the Hidden Urban Landscape of Munigua. Insights from the 2024 Ground-Penetrating Radar Survey and Its Implications for Roman and Post-Roman Occupation, MM 66, 2025, § 1–54, https://doi.org/10.34780/0h8kn659

DOI: https://doi.org/10.34780/0h8kn659
Schlagwörter/*Keyword*: Römischer Städtebau, Munigua, Georadar, Nachrömische Transformation/*Roman urbanism, Munigua, Ground-penetrating radar, Post-Roman transformation*